HHS Public Access

Author manuscript

J Neuroendocrinol. Author manuscript; available in PMC 2019 November 01.

Published in final edited form as:

J Neuroendocrinol. 2018 November ; 30(11): e12639. doi:10.1111/jne.12639.

High salt loading increases brain derived neurotrophic factor in supraoptic vasopressin neurones

Kirthikaa Balapattabi, **Joel T. Little**, **George E. Farmer**, **J. Thomas Cunningham**

Department of Physiology and Anatomy, University of North Texas Health Science Center at Fort Worth, Fort Worth, Texas

Abstract

High salt loading (SL) is associated with inappropriate arginine vasopressin (AVP) release and increased mean arterial pressure. Previous work has shown that chronic high salt intake impairs baroreceptor inhibition of rat AVP neurones through brain-derived neurotrophic factor (BDNF) dependent activation of tyrosine receptor kinase B (TrkB) and down-regulation of K+/Cl− co-transporter KCC2. This mechanism diminishes the $GABA_A$ inhibition of AVP neurones in the supraoptic nucleus (SON) by increasing intracellular chloride. However, the source of BDNF leading to this ionic plasticity is unknown. In the present study, we used adeno-associated viral vectors with short hairpin RNA against BDNF to test whether SON is the source of BDNF contributing to increased AVP release and elevated mean arterial pressure in high salt loaded rats. Virally mediated BDNF knockdown (shBDNF) in the SON of salt loaded rats significantly blocked the increases in BDNF mRNA and AVP heterogeneous RNA expression. The observed increase in the activation of TrkB receptor during salt loading is consistent with previous studies. Western blot analysis of SON punches revealed that tyrosine phosphorylation of TrkB (pTrkBY515) was significantly decreased in salt shBDNF rats compared to the salt scrambled (SCR) rats. Injections of shBDNF in the SON also significantly prevented the increase in plasma AVP concentration associated with salt loading. However, the salt loading induced increase in mean arterial pressure was not decreased with BDNF knockdown in the SON. Average daily fluid intake and urine output were significantly elevated in both salt SCR and salt shBDNF rats compared to the euhydrated controls. Daily average urine sodium concentration was significantly higher in shBDNF injected salt rats than the other groups. These findings indicate that BDNF produced in the SON contributes to the increased AVP secretion during high salt loading but not with respect to the subsequent increase in mean arterial pressure.

Keywords

BDNF; salt loading and MNCs; SON; vasopressin

Correspondence: J. Thomas Cunningham, Department of Physiology and Anatomy, UNT Health Science Center, Fort Worth, TX. tom.cunningham@unthsc.edu.

CONFLICT OF INTERESTS

The authors declare that they have no conflicts of interest.

1 | INTRODUCTION

Arginine vasopressin (AVP) is a peptide hormone that is synthesised in magnocellular neurosecretory cells (MNCs) present in the supraoptic nucleus (SON) and paraventricular nucleus (PVN) of the hypothalamus.[1–3] Arginine vasopressin is axonally transported through the hypothalamic-hypophyseal tract from hypothalamus to the posterior pituitary where it is released into systemic circulation.[1,2] The release of AVP is regulated primarily by plasma osmolality, blood pressure and blood volume.[4–6] Increased plasma osmolality activates hypothalamic MNCs increasing circulating AVP which acts at the kidneys to increase water reabsorption and maintain homeostasis. Conversely, decreased plasma osmolality is associated with inhibition of AVP MNCs, reduced plasma AVP and diuresis. A linear relationship between plasma AVP and osmolality is observed during normal conditions and requires highly coordinated excitatory and inhibitory postsynaptic responses.[3,7]

Altered synaptic homeostasis of vasopressinergic MNCs could contribute to disease conditions in which circulating AVP is abnormally elevated.[7,8] For example, congestive heart failure and decompensated cirrhosis can be associated with dilutional hyponatraemia.[9–11] The development of hyponatraemia is associated with increased morbidity and mortality in these diseases.[12–14] Despite the vast amount of knowledge available about the regulation of AVP neurones,[5,6,15–18] the pathophysiology of inappropriate AVP secretion remains unknown. Increased AVP release into systemic circulation from MNCs despite elevated mean arterial pressure (MAP) is reported during high salt loading (SL) (ie, giving rats only 2% NaCl to drink).[19] This makes salt loaded rats a suitable model for investigating changes in the neuronal regulation of AVP release as a result of chronic osmotic stress.

High salt intake causes hypernatraemia, leading to AVP release as feedback to maintain plasma osmolality. Salt-induced increases in MAP are partly mediated by AVP through the elevation of vascular resistance and renal water retention. Previous studies have shown that salt loading up-regulates brain- derived neurotrophic factor (BDNF).[19–22] Increases in BDNF diminish or reverse the $GABA_A$ mediated inhibition in AVP neurones by increasing intracellular chloride ($[Cl]_i$). This disturbance in the chloride homeostasis is mediated by BDNF- dependent activation of tyrosine receptor kinase B (TrkB) and down-regulation of potassium chloride co-transporter (KCC2). The changes in regulatory mechanisms create a feed forward loop causing sustained release of AVP and an increase in MAP.[19,21,22] However, the source of BDNF remains to be elucidated. We hypothesise that the SON is the source of BDNF contributing to increased AVP release and MAP in salt loaded rats. In the present study, we used adeno-associated viral vectors with short hairpin RNA (shRNA) against BDNF to test our hypothesis by knocking down BDNF in the SON. The findings of our study will address several critical gaps in the literature by determining the source of BDNF that contribute to neural adaptations resulting in pathophysiology of inappropriate AVP release in the high salt loaded rats.

2 | MATERIALS AND METHODS

2.1 | Animals

All of the experiments were conducted on outbred adult male Sprague-Dawley rats with a body weight of 200–250 g (Charles River, Wilmington, MA, USA). Rats were individually housed as a result of the use of survival surgery and individual fluid intake measurements in the protocol. All animals were maintained under a 12:12 hour light/dark photocycle in temperature-controlled environment with access to food and water available ad libitum unless otherwise indicated. Experimental protocols involving animals were approved by the UNT Health Science Center IACUC and were conducted in accordance with the National Institute of Health Guide for the Care and Use of Laboratory Animals. Survival surgeries were conducted using aseptic techniques. All rats were given procaine penicillin G (30 000 U, s.c.) and nonsteroidal anti-inflammatory drug, carprofen (2 mg p.o.), was given before and after surgery for pain management.

2.2 | Adeno-associated virus (AAV)-mediated knockdown of BDNF in the SON

Rats were bilaterally injected in the SON (300 nL each side) with an AAV2 serotype conjugated with a shRNA directed against BDNF, a mCherry reporter and a U6 promoter (shBDNF). Another group of rats received bilateral SON injections of equal titre and amount of AAV2 conjugated with a scrambled (SCR) sequence of shRNA (Vector Biolabs, Malvern, PA, USA) as controls. The vectors were injected at a titre of 1.0×10^{13} GC mL^{-1} (Vector Laboratories, Inc., Burlingame, CA, USA). Each rat was anaesthetised with isoflurane (2%–3%) and placed in a stereotaxic frame. Their skulls were exposed and levelled between lambda and bregma.[23] A micromanipulator was oriented to lower the probe to the targeted coordinates of SONs (1.4 mm posterior, 9.1 mm ventral and ±1.4 mm lateral from bregma). Each construct was injected in both the SONs over a 10-minute period. After 5 minutes, the injector was removed and the incision was closed with sutures.

2.3 | Metabolic cage study

After 2 weeks of recovery from surgery, rats were moved into metabolic cages (Lab Products, Seaford, DE, USA) for measurement of daily food intake, fluid intake and urine excretion. The rats were provided with ad libitum access to food and water for the first 7 days to record baseline parameters. Following the baseline measurements, a subset of shBDNF and SCR rats had their water replaced with 2% salt (NaCl) to drink for 7 days as described previously.[19] Food and fluid intake were measured by filling the containers up to a predetermined weight (g) and subtracting the remaining weight 24 hours later. Mineral oil was added to the urine collection vials to prevent evaporation of water from urine. Urine excretion volume was recorded and urine samples were collected for measuring daily sodium excretion.

2.4 | Measurement of electrolyte concentration

Urine from each rat was collected in 50-mL centrifuge tubes and a 1–2 mL aliquot was taken from each daily sample and centrifuged (10 000 *g* for 20 minutes). The sodium concentration in each of the urine samples was determined at a dilution of 1:500 using a

flame photometer (Jenway PFP7; VWR International, Radnor, PA, USA). The final sodium concentration (mmol L^{-1}) was calculated from a linear calibration curve derived from sodium standards.

2.5 | Laser capture microdissection (LCM) and quantitative real-time polymerase chain reaction (RT-PCR)

At the end of the 7-day salt loading protocol, rats were anaesthetised with inactin (100 mg kg^{-1} i.p.; Millipore, Burlington, MA, USA) and decapitated. Their brains were collected and flash frozen using precooled two-methyl butane. Fresh frozen brains were prepared for LCM[18,20] by cutting coronal sections (thickness 10 μm) through the hypothalamus at the level of the SON. The sections were mounted onto poly(*p*-phenylene) sulphide membrane coated slides (Leica Microsystems, Buffalo Grove, IL, USA). Separate sets of sections (thickness 40 μm) were mounted on gel coated slides to verify the histology of other nuclei in hypothalamus. A laser capture microdissection instrument (Leica Microsystems), which utilises an ultraviolet cutting laser to dissect the region of interest into a collection tube, was used to confirm the accuracy of the injection sites by visualising the mCherry reporter and to specifically collect the SON neurones. A minimum of seven to nine SON regions was laser captured and collected from each rat for RNA extraction and amplification. The SONs collected by LCM were used to measure changes in BDNF mRNA and AVP heterogeneous RNA (hnRNA) using quantitative RT-PCR. The RNA was extracted and purified from each sample using ArrayPure Nano-Scale RNA Purification Kit reagents (Epicentre Biotechnologies, Madison, WI, USA). The concentration and quality of each RNA sample was evaluated using a Nanodrop Spectrophotometer (Thermo Fisher Scientific Inc., Waltham, MA, USA) and reverse transcribed to cDNA with Sensiscript RT Kit reagents (Qiagen, Valencia, CA, USA).[20] Real-time PCR was performed on an CFX96 C1000 Cycler (Bio-Rad, Hercules, CA, USA) with SYBR green fluorescence labelling. Samples (final volume of 15 μL) contained: SYBR green master mix (Bio-Rad), 3–5 pmol of each primer and an equal concentration of cDNA. Cycling parameters were: 95°C for 3 minutes, then 40 cycles of 95°C for 10 seconds and 60°C for 1 minute. A melting temperature-determining dissociation step was performed from 65°C to 95°C at increments of 0.5°C every 5 seconds at the end of the amplification phase.

Forward and reverse primers for target genes (Table 1) were obtained from Integrated DNA Technologies (Coralville, IA, USA). The housekeeping gene S18 was used to normalise RNA expression.Melt curves generated were analysed to identify nonspecific products and primer-dimers. The data were analysed by the $2^{-\Delta\Delta Ct}$ method.[24,25] ΔC_t was measured by calculating the difference between the S18 and the corresponding gene of interest C_t values. To obtain the $\Delta\Delta C_t$ value, this value was then subtracted from the difference between the average of control S18 and control gene of interest C_t values.[18,26,27]

2.6 | Plasma measurements

Trunk blood (1–2 mL) was collected from each rat after decapitation and prepared for measuring plasma osmolality and haematocrit as described previously.[18] Plasma osmolality was measured on a vapor pressure osmometer (Wescor, Logan, UT, USA). Two heparinised

capillary tubes (Fisher Scientific, Hampton, NH, USA) were filled for measuring haematocrit using a micro-haematocrit capillary tube reader (Lancer, St Louis, MO, USA).

Further blood (5–6 mL) was collected in Vacutainer tubes (Becton-Dickinson Biosciences, Franklin Lakes, NJ, USA) containing the anticoagulant ethylenediaminetetraacetic acid (12 mg). The proteinase inhibitor, aprotinin (0.6 TIU mL^{-1} of blood; Phoenix Pharmaceuticals, Inc., Burlingame, CA, USA) was added and the sample was centrifuged at 1600 *g* for 15 minutes at 4°C. A sample of plasma (2–3 mL) was removed from each sample and peptides were extracted from plasma by solid phase extraction using a C-18 SEP-Column (Phenomenex, Torrance, CA, USA). After extraction, each sample was subjected to vacuum centrifugal concentration. Circulating AVP concentration was measured using a specific enzyme-linked immunosorbent assay in accordance with the manufacturer's instructions (EK-065–07; Phoenix Pharmaceuticals, Inc.). Four parametric logistic analysis was performed to quantify the concentration of peptide.

2.7 | Western blot analysis

At the end of 7-day salt loading protocol, the rats were anaesthetised with inactin (100 mg kg^{-1} i.p.) and decapitated. Punches containing the SON were collected from a 1-mm coronal section from each brain as described previously.[18,28] Protein was extracted from the SON punches using RIPA lysis buffer containing dithiotreitol, chelators and protease phosphatase inhibitor cocktail. Protein concentration was determined by the BCA assay with varying concentrations of bovine serum albumin (BSA) as reference standards. Total lysate (20–25 μg) was loaded onto a 4%−15% acrylamide sodium dodecyl sulphate (SDS) gel and separated by electrophoresis in Tris-glycine buffer with denaturing conditions. The protein was transferred to a polyvinylidene difluoride membrane (Immobilon-P; Millipore) in Tris-glycine buffer (25 mmol L^{-1} Tris, 192 mmol L^{-1} glycine, 0.1% SDS; pH 8.3) with 20% (v/v) methanol. Membranes were blocked with 5% BSA in Tris-buffered saline-Tween 20 (25 mmol L^{-1} Tris base, 125 mmol L^{-1} NaCl, 0.1% Tween 20) for 30 minutes at room temperature. The membranes were incubated with primary antibodies made in 5% BSA overnight at 4°C. The primary antibodies used were: phosphorylated TrkB (Y515; rabbit polyclonal; dilution 1:1000; ab109684; Abcam, Cambridge, MA, USA); total TrkB (goat; dilution 1:1000; GT15080; Neuromics, Edina, MN, USA); phosphorylated KCC2 (Ser940; rabbit polyclonal; dilution 1:500; 612–401-E15; Rockland Immunochemicals, Inc., Pottstown, PA, USA); mCherry (rabbit polyclonal; dilution 1:500; ab167453; Abcam); and GAPDH (mouse monoclonal; dilution 1:2000; MAB374; Millipore).

Membranes were rinsed three times at 10-minute intervals with TBS-Tween followed by a 2-hour incubation at room temperature with a horseradish peroxidase-conjugated secondary antibody against the primary antibody host species (anti-rabbit, anti-goat, or anti-mouse; dilution 1:1000; Sigma, St Louis, MO, USA). The membranes were washed three times at 5-minute intervals with TBS-Tween. Proteins were visualised using an enhanced chemiluminescence substrate kit (Supersignal West Femto Maximum Sensitivity kit; Thermo Fisher Scientific Inc.). Blots were developed, and the digital image was obtained using GBOX in GENESNAP (Syngene, Fredrick, MD, USA) and densitometry analysis of the

bands was performed using IMAGEJ (NIH, Bethesda, MD, USA). Densitometry measurements of the immunoreactive bands were normalised using GAPDH as a loading control.

2.8 | Mean arterial pressure (MAP) and heart rate measurements using radio telemetry

After 1 week of recovery from stereotaxic injections, some rats from each group were instrumented with radio telemetry transmitters (TA11PA-C40 telemetry unit; Data Science International, St Paul, MN, USA) under isoflurane anaesthesia (2%−3%) as described previously.[29] The blood pressure catheter was advanced into the abdominal aorta and the radio transmitter device was placed in the peritoneal cavity for the duration of the experiment. Direct recording of MAP, heart rate and activity was performed using transmitters. After 2 weeks of recovery, signals from the telemetry device were recorded for 7-day baseline followed by 7-day SL using a Dataquest IV radio telemetry system (Data Sciences International). During the experiments, heart rate, activity and MAP were all measured for 10 seconds every 10 minutes for 24 h d^{-1} and averaged as described previously.[29]

2.9 | Statistical analysis

In all of the above experiments, the rats were divided into four groups: (i) euhydrated rats injected with SCR virus (Eu SCR); (ii) euhydrated rats injected with shBDNF virus (Eu shBDNF); (iii) salt loaded rats injected with SCR virus (Salt SCR); and (iv) Salt loaded rats injected with shBDNF virus (Salt shBDNF).

Data from the metabolic cage studies and electrolyte measurements were analysed by separate two-way repeated measures ANOVA with time as first factor and treatment (drinking fluid with stereotaxic injection) as second factor, followed by Bonferroni post-hoc tests. All other data were analysed using one-way ANOVA with Bonferroni post-hoc tests using SIGMA PLOT, version 12.0 (Systat Software Inc., Chicago, IL, USA). Images were assembled using the ‘magick’ package in RSTUDIO (Rstudio Inc., Boston, MA, USA). The group sizes were determined by power analysis and effect size as calculated from our previous work[16,18,19] and preliminary data using SIGMA PLOT, version 12.0. Power analysis calculation elements included considerations of $P < 0.05$, α of 0.8, largest difference between means, and the largest SD observed from our studies. The Eta^2 (η^2) method was chosen to calculate the effect sizes, and the sample sizes were balanced (equal) in all the groups and were independent of each other. Sum of squares of effect and the total from our previous studies[15,16,18,19] were used for effect size determination. The minimal numbers per group for each experiment was determined to achieve an appropriately powered study with an effect size (η^2) of approximately 0.7 (70%). Data are reported as the mean ± SEM.

3 | RESULTS

3.1 | Changes in AVP and BDNF gene expression in the SON

Using LCM, we verified the accuracy of the stereotaxic injections by visualising the mCherry reporter (Figure 1A) and collected the SONs to measure changes in the BDNF mRNA and AVP hnRNA expression using quantitative RT-PCR by the $2^{-\Delta\Delta Ct}$ method. Rats that did not have successful virus injections in the SON were analysed separately. One-way

ANOVA revealed significant difference between the groups in BDNF ($F_{3,23} = 5.78$, $P < 0.05$) and AVP ($F_{3,23} = 8.83$, $P < 0.05$) gene expression. Bonferroni post-hoc analysis showed that salt loading significantly increased BDNF and AVP gene expression in the SON of rats injected with SCR compared to the euhydrated rats (Bonferroni *t* tests, all $P < 0.05$) (Figure 1). Post-hoc multiple comparison of mRNA levels between Salt SCR and Salt shBDNF groups showed that SON injections of shBDNF significantly blocked the increases in BDNF mRNA (Bonferroni $t = 3.310$, $P < 0.05$) and AVP hnRNA (Bonferroni $t = 4.09$, $P < 0.05$) in the SON of salt loaded rats. In rats with injections of shBDNF outside of the SON, salt loading significantly increased BDNF mRNA in the SON ($F_{3,12} = 7.33$, $P < 0.05$) (Figure 2) and the increase produced by salt loading was not different compared to the Salt SCR group (Bonferroni $t = 0.37$, $P > 0.05$) (Figure 2).

3.2 | Changes in phosphorylation of TrkB and KCC2 in the SON

We used mCherry expression to verify the specificity of stereotaxic injections (Figure 3). One-way ANOVA analysis revealed significant difference between the groups in TrKB phosphorylation ($F_{3,23} = 6.778$, $P < 0.05$) and KCC2 phosphorylation ($F_{3,24} = 4.546$, $P < 0.05$). Seven days of 2% salt loading significantly increased TrkB phosphorylation without affecting total TrkB expression and decreased phosphorylation of KCC2 (Bonferroni *t* tests, all $P < 0.05$) (Figure 3) in the SON of rats injected with the control vector compared to the euhydrated rats. Virally mediated BDNF knockdown in the SON of salt loaded rats significantly prevented the increase in TrkB phosphorylation and decrease in KCC2 phosphorylation compared to euhydrated rats (Bonferroni *t* tests, all $P < 0.05$) (Figure 3). One to two rats in each group did not have successful virus injections in the SON, as confirmed at the end of the experiment using either LCM/quantitative RT-PCR or western blot analysis, and the results were excluded from the data analysis in all of the subsequent experiments.

3.3 | Changes in fluid intake, urine excretion, food intake and body weight

Fluid intake was measured daily before and during 7 days of 2% salt loading. Two-way repeated measures ANOVA revealed a significant interaction indicating that fluid intake was affected by time and the treatment protocol (Time × Treatment $F_{39,351} = 18.44$, $P < 0.001$) (Figure 4A). Post-hoc multiple comparisons between the factors revealed that, although there were no differences among the groups during baseline, salt loading significantly increased fluid intake and this increase was not affected by BDNF knockdown in the SON. Similar results were obtained for urine excretion (Time × Treatment $F_{39,351} = 24.419$, $P < 0.001$) (Figure 4B) and food intake (Time × Treatment $F_{39,351} = 18.420$, $P < 0.001$) (Figure 4C). The average daily urine volume during baseline was not different among the groups and salt loading increased urine output comparably in both Salt SCR and Salt shBDNF rats (Figure 4B). Food intake was significantly decreased in both groups of salt loaded rats compared to the euhydrated rats (Figure 4C). Concomitantly, the average body weight increase during salt loading was significantly decreased in both Salt SCR and Salt shBDNF rats compared to the euhydrated rats ($F_{3,36} = 27.48$, $P < 0.001$; Bonferroni *t* tests, $P < 0.05$) (Figure 4D).

3.4 | Changes in electrolyte excretion

Urine sodium excretion was measured before and during the 7-day salt loading protocol. Average daily changes in sodium excretion were significantly affected by time and the treatment protocol ($F_{39,312} = 35.65$, $P < 0.001$) (Figure 5A). There were no differences among the groups during baseline. During salt loading, daily average change in sodium excretion significantly increased in the Salt SCR rats compared to the two euhydrated control groups (Bonferroni *t* tests, all $P < 0.05$) (Figure 5A). The daily changes in sodium excretion following BDNF knockdown in the SON were significantly increased during the 7-day salt loading compared to all the other groups (Bonferroni *t* tests, $P < 0.05$) (Figure 5A). Knockdown of BDNF in the SON also significantly increased total average daily sodium concentration ($F_{3,32} = 43.55$, $P < 0.001$) (Figure 5B). The average daily urine sodium concentrations of salt loaded rats were significantly higher than the euhydrated groups during salt treatment. In addition, the Salt shBDNF group showed significantly higher urine sodium excretion than the Salt SCR rats (Bonferroni *t* tests, all $P < 0.05$) (Figure 5B).

3.5 | Changes in plasma AVP, osmolality and volume

One-way ANOVA revealed significant difference between the groups in plasma AVP concentration ($F_{3,18} = 26.227$, $P < 0.05$). Bonferroni multiple comparisons show that rats with SCR injections and salt loading had significantly increased circulating AVP compared to all the other groups (Bonferroni *t* tests, all $P < 0.001$) (Table 2). Knockdown of BDNF in the SON of salt loaded rats significantly decreased plasma AVP compared to the Salt SCR group (Bonferroni $t = 6.661$, $P < 0.05$) (Table 2). Plasma osmolality and haematocrit values were significantly different between the groups (plasma osmolality $F_{3,47} = 20.746$, $P < 0.001$; hematocrit $F_{3,47} = 18.478$, $P < 0.001$). The Salt SCR rats also had plasma osmolality and haematocrit values that were significantly higher than all other groups (Bonferroni *t* tests, all $P < 0.05$). The Salt shBDNF group had significantly lower plasma osmolality (Bonferroni $t = 4.146$, $P < 0.05$) (Table 2) and haematocrit (Bonferroni $t = 3.708$, $P < 0.05$) (Table 2) compared to the Salt SCR group.

3.6 | Changes in MAP and heart rate

Two-way repeated measures ANOVA revealed a significant interaction indicating that MAP was affected by time and the treatment protocol (Time × Treatment $F_{39,312} = 21.169$, $P < 0.001$) (Figure 6). Post-hoc multiple comparisons between the factors revealed that there were no differences among the groups during baseline (Table 3). Salt loading was associated with significant increases in MAP in rats injected in the SON with either SCR or shBDNF. The MAP increases in the two salt loaded groups were not different from each other (Figure 6A, B). Two-way repeated measures ANOVA followed by post-hoc analysis show that salt loading was associated with a significant decrease in heart rate (Time × Treatment $F_{39,312} = 3.221$, $P < 0.001$) (Figure 6C, D and Table 3) that was no different between the SCR and shBDNF injected rats.

4 | DISCUSSION

AVP MNCs are regulated by negative-feedback from arterial baroreceptors mediated by $GABA_A$ inhibition.[6,21] Previous studies have established that chronic salt loading can impair this baroreceptor inhibition by altering chloride homeostasis of MNCs through a BDNF-TrkB signalling mechanism.[19–21] It is important to identify the source of BDNF leading to changes in the regulatory mechanism to obtain a complete understanding of the pathophysiology of inappropriate AVP release. The results of the present study show that the SON is the source of BDNF resulting in an inappropriate release of AVP in salt loaded rats.

Circulating AVP is primarily determined by the activity of MNCs located in the PVN and SON of the hypothalamus.[3,16] In addition, MNCs are reported to express both BDNF and TrkB.[20] Because SON is less heterogeneous than PVN and we previously observed salt loading-mediated changes in GABA inhibition of SON MNCs, we injected an AAV vector constructed with shRNA against BDNF (AAV2-U6-shBDNF) bilaterally into the SON. This specific knockdown approach helped determine whether increased expression of BDNF in the SON contributes to the elevated circulating AVP shBDNF viral construct have shown that its effects are primarily neurotrophic and that it produces stable knockdown of BDNF.[19]

Knocking down BDNF in the SON of salt loaded rats significantly attenuated the increases in AVP hnRNA in the SON and circulating AVP normally associated with salt loading. Chronic salt intake increased the concentration of plasma sodium and proportionally increased plasma osmolality. Knockdown of BDNF in the SON was also associated with a significant decrease in plasma osmolality and a significant increase in sodium excretion. Blocking the increase in BDNF in the SON produced natriuresis in salt loaded rats that may have contributed to the observed decrease in plasma osmolality. It is likely the natriuesis is related to the decrease in circulating AVP,[30] although this was not tested. Elevation of plasma osmolality by salt loading can activate hypothalamic oxytocin neurones. An additional possibility is that oxytocin can facilitate the release of atrial natriuretic peptide, which reduces an expanded extracellular fluid volume by increasing urine and renal sodium excretion.[4,31]

Injections of shBDNF in the SON did not cause any changes in the volume of urine excretion or fluid and food intake behavior. Food intake and body weight in salt loaded groups were significantly decreased compared to the euhydrated groups. High salt intake caused the rats to decrease food intake and subsequently reduced body weight.[32]

Although BDNF knockdown in the SON significantly attenuated AVP release in salt loaded rats, it did not similarly influence MAP. In the present study, MAP was significantly increased in the salt loaded groups compared to the euhydrated groups in accordance with previous studies.[19] These data indicate that mechanisms other than those involving AVP from the SON could contribute to the observed increase in MAP during high salt loading. Moreover, studies have shown that recruitment of central osmoreceptor pathways enhances sympathetic tone through excitation of preautonomic neurones.[19,33] Another factor that could have influenced these results is the experimental protocol. The AAV treatments were applied only to the SON. AVP dendritically released from magnocellular secretory neurones

in the PVN has been shown to increase sympathetic outflow.[34] This mechanism would not have been influenced by the AAV injections in the SON and could still contribute to the increase in MAP associated with salt loading. Also, BDNF knockdown was induced before the rats were exposed to salt loading. This was carried out because the time required to allow the AAV to transfect the cells in the SON is longer than the 7-day salt loading protocol. As noted above, this protocol significantly reduced AVP release, although it did not prevent the increase in MAP. It could be that mechanisms related to autonomic function, which do not depend on the SON, were able to compensate for the lack of AVP release. Inhibiting BDNF-TrkB signalling in the SON during the 7-day salt loading protocol could possibly prevent the increase in MAP.

The results of the present study show that increased BDNF expression in the SON during chronic salt loading leads to TrkB receptor activation as indicated by increased tyrosine (Y^{515}) phosphorylation. In most neurones, the low $[Cl]_i$ required for the $GABA_A$ synaptic inhibition is a result of relative activity of KCC2 and/or NKCC1 ($Na+/K^+/Cl^-$ co-transporter) membrane co-transporters. In the SON, salt loading was associated with decreased serine (S^{940}) phosphorylation of KCC2. Decreased phosphorylation of KCC2 at this residue is associated with translocation of the protein from the membrane and functional loss of its chloride transport activity.[35–37] This could be the mechanism responsible for the change in the va-lance of the $GABA_A$ in the SON produced by salt loading. However, the proposed changes in membrane expression of KCC2 in the SON and its effect on $[Cl]_i$ remain to be investigated.

Other studies have suggested that changes in the function of NKCC1 also modulate the valence of $GABA_A$ on MNCs in the SON.[38,39] There are several different signalling pathways that influence the function of both KCC2 and NKCC1 and potentially impact GABAergic function.[40,41] Although the results of the present study show that salt loading induced activity-dependent mechanisms can affect KCC2 phosphorylation, the role of post-translational mechanisms with respect to controlling KCC2 expression, specifically at the cell surface, are poorly understood. However, the cellular mechanisms by which changes in Cl^- homeostasis affect the GABA-mediated feedback inhibition in MNCs have not been resolved yet.

The result of the present study indicate that the SON neurones themselves are the source of BDNF causing dysregulation of AVP neurones during salt loading. However, we cannot conclude whether the source is AVP or oxytocin or both the SON neurones. Therefore, BDNF could have autocrine or paracrine effects in the SON that change the phosphorylation status of KCC2. This would change the valence of the GABA response of AVP neurones to baroreceptor stimulation as reported previously.[19] However, BDNF knockdown in the SON was not sufficient to prevent the salt loading induced increase in MAP.

The present study advances our understanding about the pathophysiology of AVP neurone regulation. Identifying the source of BDNF underlying the changes in postsynaptic inhibition of AVP neurones in response to salt loading may result in novel strategies for reducing AVP secretion in other pathological states, such as heart and liver failure.[9,16,42]

This would provide a novel therapeutic target for the treatment of inappropriate AVP release and its associated morbidities.

ACKNOWLEDGEMENTS

The authors thank M. Bachelor and Dr L. A. Wang for their assistance.

Funding information

This work was supported by R01 HL119458 to JTC and AHA18PRE34060035 to KB.

REFERENCES

1. Cunningham JT, Penny ML, Murphy D. Cardiovascular regulation of supraoptic neurons in the rat: synaptic inputs and cellular signals. Prog Biophys Mol Biol. 2004;84:183–196. [PubMed: 14769435]
2. Armstrong WE. Morphological and electrophysiological classification of hypothalamic supraoptic neurons. Prog Neurobiol. 1995;47:291–339. [PubMed: 8966209]
3. Di S, Tasker JG. Dehydration-induced synaptic plasticity in magnocellular neurons of the hypothalamic supraoptic nucleus. Endocrinology. 2004;145:5141–5149. [PubMed: 15297447]
4. Gizowski C, Bourque CW. The neural basis of homeostatic and anticipatory thirst. Nat Rev Nephrol. 2017;14:11. [PubMed: 29129925]
5. Bourque CW. Central mechanisms of osmosensation and systemic osmoregulation. Nat Rev Neurosci. 2008;9:519–531. [PubMed: 18509340]
6. Verbalis JG. Osmotic inhibition of neurohypophysial secretion. Ann NY Acad Sci. 1993;689:146–160. [PubMed: 8373011]
7. Leng G, Brown CH, Bull PM, et al. Responses of magnocellular neurons to osmotic stimulation involves coactivation of excitatory and inhibitory input: an experimental and theoretical analysis. J Neurosci. 2001;21:6967–6977. [PubMed: 11517284]
8. Potapenko ES, Biancardi VC, Zhou Y, Stern JE. Astrocytes modulate a postsynaptic NMDA-GABAA-receptor crosstalk in hypothalamic neurosecretory neurons. J Neurosci. 2013;33:631–640. [PubMed: 23303942]
9. Braun MM, Barstow CH, Pyzocha NJ. Diagnosis and management of sodium disorders: hyponatremia and hypernatremia. Am Fam Physician. 2015;91:299–307. [PubMed: 25822386]
10. Iovino M, Iacoviello M, De Pergola G, et al. Vasopressin in heart failure. Endocr Metab Immune Disord Drug Targets. 2018;18:458–465. [PubMed: 29437026]
11. Verbalis JG. Disorders of body water homeostasis. Best Pract Res Clin Endocrinol Metab. 2003;17:471–503. [PubMed: 14687585]
12. Boscoe A, Paramore C, Verbalis JG. Cost of illness of hyponatremia in the United States. Cost Eff Resour Alloc. 2006;4:10. [PubMed: 16737547]
13. Corona G, Giuliani C, Parenti G, et al. Moderate hyponatremia is associated with increased risk of mortality: evidence from a meta-analysis. PLoS ONE. 2013;8:e80451. [PubMed: 24367479]
14. Oren RM. Hyponatremia in congestive heart failure. Am J Cardiol.2005;95:2–7.
15. Carreño FR, Ji LL, Cunningham JT. Altered central TRPV4 expression and lipid raft association related to inappropriate vasopressin secretion in cirrhotic rats. Am J Physiol Regul Integr Comp Physiol. 2009;296:R454–R466. [PubMed: 19091909]
16. Cunningham JT, Nedungadi TP, Walch JD, Nestler EJ, Gottlieb HB. ΔFosB in the supraoptic nucleus contributes to hyponatremia in rats with cirrhosis. Am J Physiol Regul Integr Comp Physiol. 2012;303:R177–R185. [PubMed: 22621966]
17. Cunningham JT, Nissen R, Renaud LP. Norepinephrine injections in diagonal band of Broca selectively reduced the activity of vasopressin supraoptic neurons in the rat. Brain Res. 1993;610:152–155. [PubMed: 8518923]

18. Nedungadi TP, Cunningham JT. Differential regulation of TRPC4 in the vasopressin magnocellular system by water deprivation and hepatic cirrhosis in the rat. Am J Physiol Regul Integr Comp Physiol. 2014;306:R304–R314. [PubMed: 24352411]
19. Choe KY, Han SY, Gaub P, et al. High salt intake increases blood pressure via BDNF-mediated downregulation of KCC2 and impaired baroreflex inhibition of vasopressin neurons. Neuron. 2015;85:549–560. [PubMed: 25619659]
20. Carreno FR, Walch JD, Dutta M, Nedungadi TP, Cunningham JT. Brain-derived neurotrophic factor-tyrosine kinase B pathway mediates NMDA receptor NR2B subunit phosphorylation in the supra-optic nuclei following progressive dehydration. J Neuroendocrinol. 2011;23:894–905. [PubMed: 21848649]
21. Choe KY, Trudel E, Bourque CW. Effects of salt loading on the regulation of rat hypothalamic magnocellular neurosecretory cells by Ionotropic GABA and glycine receptors. J Neuroendocrinol. 2016;28:22–23. 10.1111/jne.12372
22. Marosi K, Mattson MP. Hold the salt: vasopressor role for BDNF. Cell Metab. 2015;21:509–510. [PubMed: 25863241]
23. Paxinos G, Watson C. The Rat Brain in Stereotaxic Coordinates San Diego, CA: Academic Press; 1997.
24. Livak KJ, Schmittgen TD. Analysis of relative gene expression data using real-time quantitative PCR and the 2(-Delta Delta C(T)) Method. Methods. 2001;25:402–408. [PubMed: 11846609]
25. Schmittgen TD, Livak KJ. Analyzing real-time PCR data by the comparative C(T) method. Nat Protoc. 2008;3:1101–1108. [PubMed: 18546601]
26. Walch JD, Carreño FR, Cunningham JT. Intracerebroventricular losartan infusion modulates angiotensin type 1 receptor expression in the subfornical organ and drinking behaviour in bile duct ligated rats. Exp Physiol. 2013;98:922–933. [PubMed: 23243146]
27. Walch JD, Nedungadi TP, Cunningham JT. ANG II receptor subtype 1a gene knockdown in the subfornical organ prevents increased drinking behavior in bile duct-ligated rats. Am J Physiol Regul Integr Comp Physiol. 2014;307:R597–R607. [PubMed: 25009217]
28. Nedungadi TP, Carreno FR, Walch JD, Bathina CS, Cunningham JT. Region specific changes in TRPV channel expression in the vasopressin magnocellular system in hepatic cirrhosis induced hyponatremia. J Neuroendocrinol. 2012;24:642–652. [PubMed: 22188460]
29. Cunningham JT, Knight WD, Mifflin SW, Nestler EJ. An essential role for DeltaFosB in the median preoptic nucleus in the sustained hypertensive effects of chronic intermittent hypoxia. Hypertension. 2012;60:179–187. [PubMed: 22689746]
30. Kortenoeven MLA, Pedersen NB, Rosenbaek LL, Fenton RA. Vasopressin regulation of sodium transport in the distal nephron and collecting duct. Am J Physiol Renal Physiol. 2015;309:F280–F299. [PubMed: 26041443]
31. Mecawi Ade S, Ruginsk SG, Elias LL, Varanda WA, Antunes-Rodrigues J. Neuroendocrine regulation of hydromineral homeostasis. Compr Physiol. 2015;5:1465–1516. [PubMed: 26140725]
32. Watts AG, Boyle CN. The functional architecture of dehydration-anorexia. Physiol Behav. 2010;100:472–477. [PubMed: 20399797]
33. Toney GM, Stocker SD. Hyperosmotic activation of CNS sympathetic drive: implications for cardiovascular disease. J Physiol. 2010;588:3375–3384. [PubMed: 20603334]
34. Son SJ, Filosa JA, Potapenko ES, et al. Dendritic peptide release mediates interpopulation crosstalk between neurosecretory and preautonomic networks. Neuron. 2013;78:1036–1049. [PubMed: 23791197]
35. Zhao B, Wong AY, Murshid A, Bowie D, Presley JF, Bedford FK. Identification of a novel di-leucine motif mediating K(+)/Cl(−) cotransporter KCC2 constitutive endocytosis. Cell Signal. 2008;20:1769–1779. [PubMed: 18625303]
36. Wright R, Newey SE, Ilie A, et al. Neuronal chloride regulation via KCC2 is modulated through a GABAB receptor protein complex. J Neurosci. 2017;37:5447–5462. [PubMed: 28450542]
37. Hewitt SA, Wamsteeker JI, Kurz EU, Bains JS. Altered chloride homeostasis removes synaptic inhibitory constraint of the stress axis. Nat Neurosci. 2009;12:438–443. [PubMed: 19252497]

38. Kim JS, Kim WB, Kim YB, et al. Chronic hyperosmotic stress converts GABAergic inhibition into excitation in vasopressin and oxytocin neurons in the rat. J Neurosci. 2011;31:13312–13322. [PubMed: 21917814]

39. Kim YB, Kim YS, Kim WB, et al. GABAergic excitation of vasopressin neurons: possible mechanism underlying sodium-dependent hyper-tension. Circ Res. 2013;113:1296–1307. [PubMed: 24103391]

40. Kaila K, Price TJ, Payne JA, Puskarjov M, Voipio J. Cation-chloride cotransporters in neuronal development, plasticity and disease. Nat Rev Neurosci. 2014;15:637–654. [PubMed: 25234263]

41. Kahle KT, Delpire E. Kinase-KCC2 coupling: Cl-rheostasis, disease susceptibility, therapeutic target. J Neurophysiol. 2016;115:8–18. [PubMed: 26510764]

42. Better OS, Aisenbrey GA, Berl T, et al. Role of antidiuretic hormone in impaired urinary dilution associated with chronic bile-duct ligation. Clin Sci (Lond). 1980;58:493–500. [PubMed: 7428281]

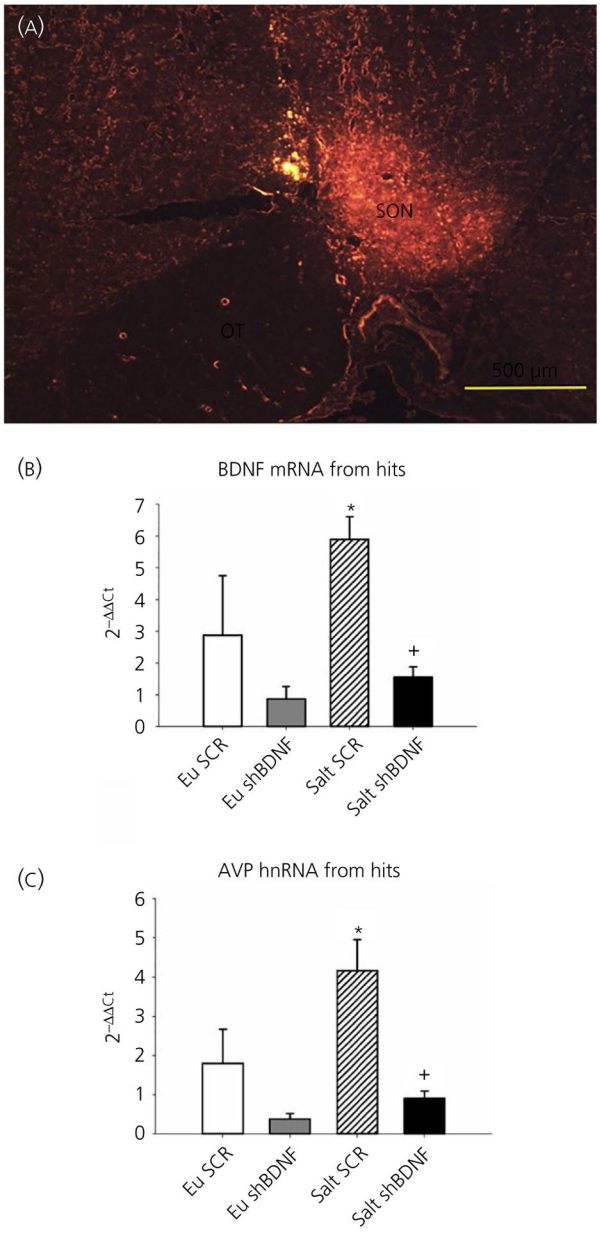

FIGURE 1.

A,Representative digital image of mCherry fluorescence in the supraoptic nucleus (SON) illustrating a successful injection. B, Quantitative reverse transcriptase-polymerase chain reaction data showing brain-derived neurotrophic factor (BDNF) mRNA expression from the SON of rats with successful SON injections. C, Arginine vasopressin (AVP) heterogeneous RNA expression from the SONs of rats with successful SON injections. Groups: euhydrated rats injected with scrambled (SCR) virus (Eu SCR, n = 6); euhydrated rats injected with shBDNF virus (Eu shBDNF, n = 7); salt loaded rats injected with SCR virus (Salt SCR, n = 7) and salt loaded rats injected with shBDNF virus (Salt shBDNF, n = 7). Data are the mean ± SEM. $^{*}P < 0.05$ vs all other groups.$^{+}P < 0.05$ vs Salt SCR. OT, optic tract

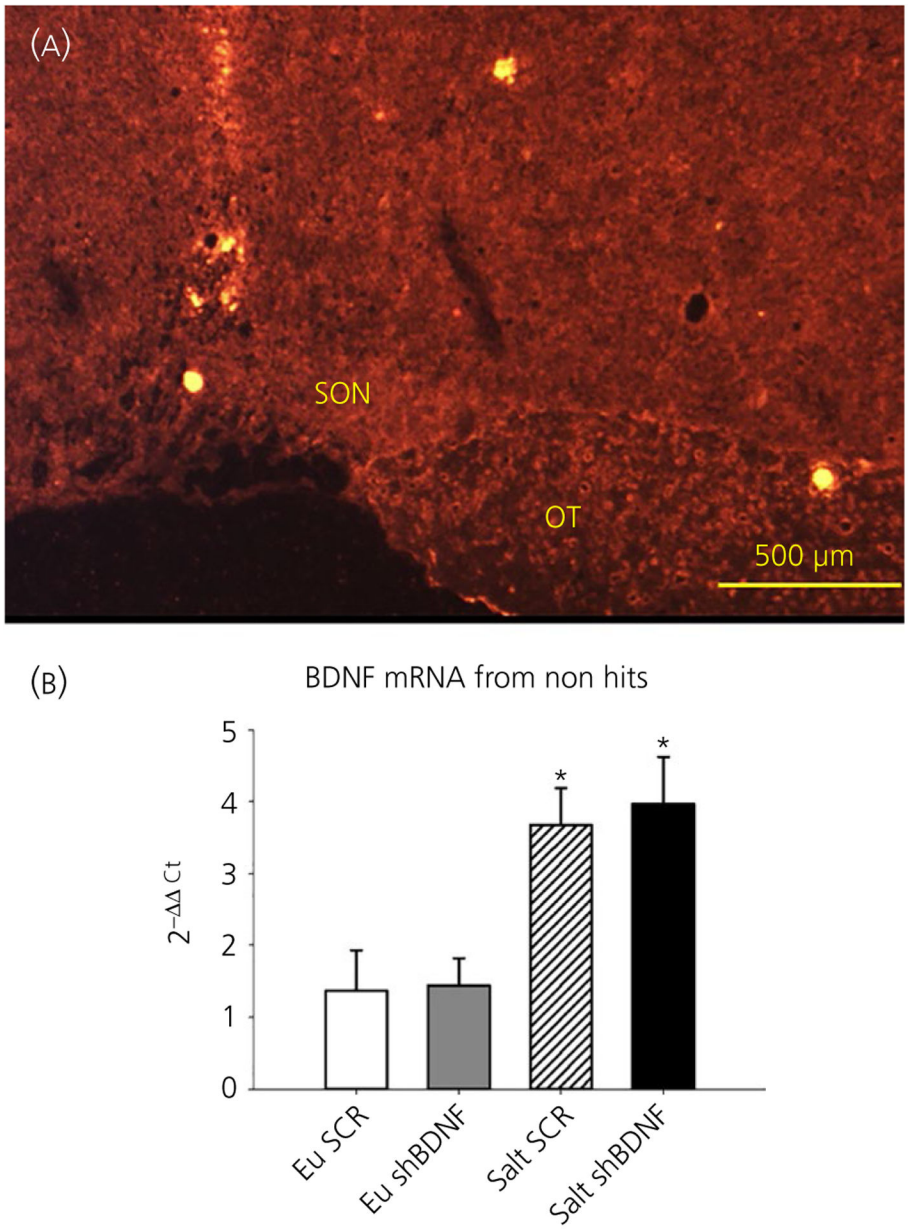

FIGURE 2.

A, Example of missed injection. mCherry fluorescence is not seen in the supraoptic nucleus (SON) as the viral injection did not include the SON. B, Brain-derived neurotrophic factor (BDNF) RNA from the SONs of rats with injections that did not include the SON. Groups: euhydrated rats injected with scrambled (SCR) virus (Eu SCR, n = 4); euhydrated rats injected with shBDNF virus (Eu shBDNF, n = 5); salt loaded rats injected with SCR virus (Salt SCR, n = 4) and salt loaded rats injected with shBDNF virus (Salt shBDNF, n = 3). Data are the mean ± SEM.* $P < 0.05$ vs Eu groups. OT, optic tract

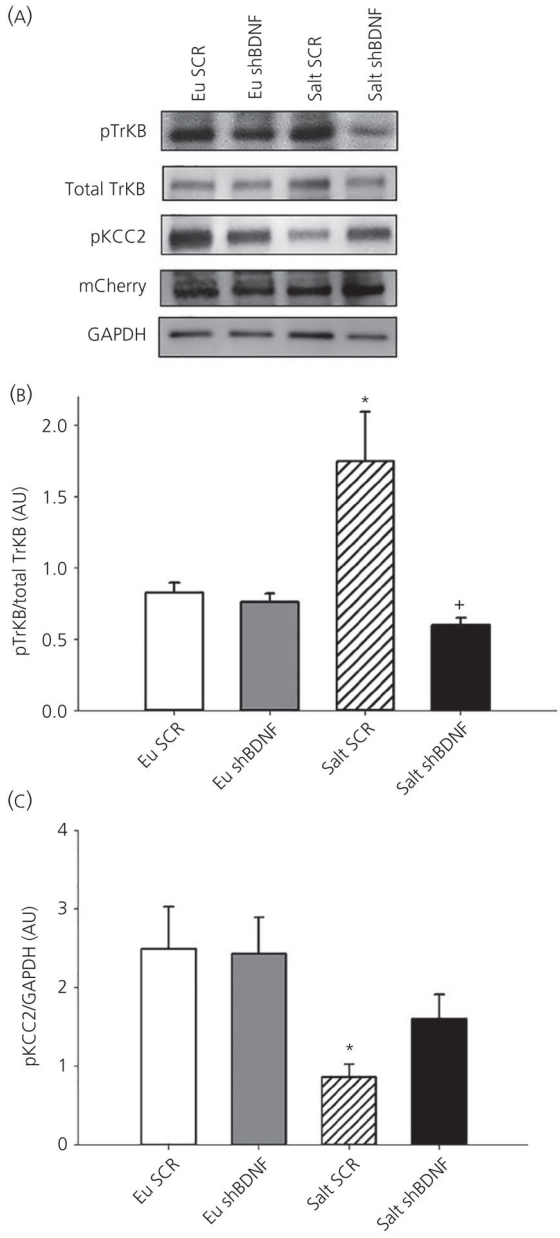

FIGURE 3.

A, Sample western blot images showing changes in protein expression of supraoptic nucleus (SON) punches. mCherry protein expression images shows successful injections at SON B, Quantification of phosphorylated tyrosine receptor kinase B (TrkB) (normalised to total TrkB). Data are the mean ± SEM. $*P < 0.05$ vs all other groups. $^{+}P < 0.05$ vs salt scrambled (SCR). C, Phosphorylated KCC2 normalised to GAPDH. $*P < 0.05$ vs all other groups. Groups: euhydrated rats injected with SCR virus (Eu SCR, n = 6); euhydrated rats injected with shBDNF virus (Eu shBDNF, n = 6); salt loaded rats injected with SCR virus (Salt SCR, n = 8) and salt loaded rats injected with shBDNF virus (Salt shBDNF, n = 8)

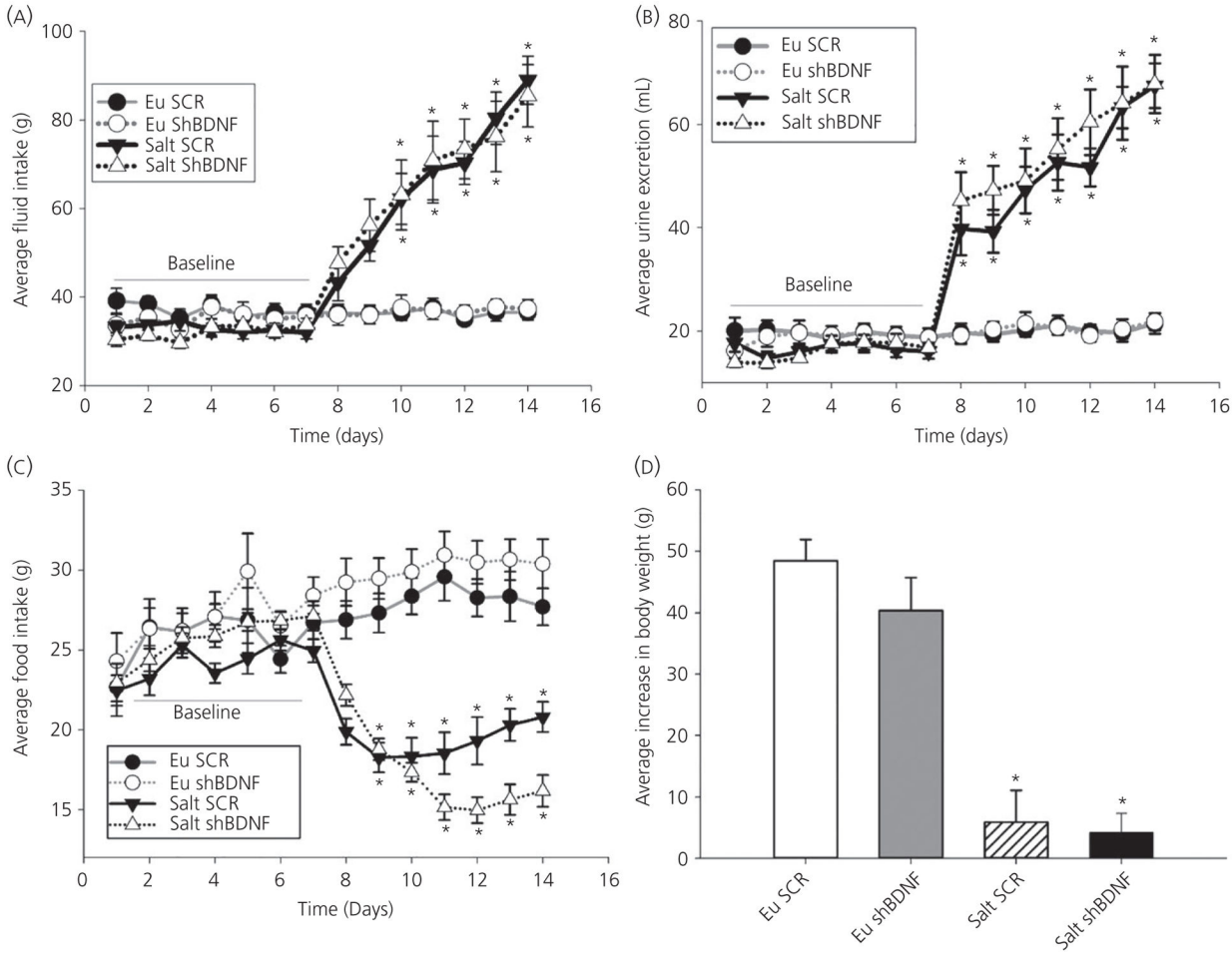

FIGURE 4.

The effects of salt loading and brain-derived neurotrophic factor (BDNF) knockdown in the supraoptic nucleus (SON). A, Daily average fluid intake. B, Daily average urine excretion. C, Daily average food intake. A-C, **P* < 0.05 vs euhydrated (Eu) groups and vs baseline. D, Average daily changes in body weight. Data are the mean ± SEM. **P* < 0.05 vs Eu groups. Groups: euhydrated rats injected with scrambled (SCR) virus (Eu SCR, n = 8); euhydrated rats injected with shBDNF virus (Eu shBDNF, n = 8); salt loaded rats injected with SCR virus (Salt SCR, n = 8) and salt loaded rats injected with shBDNF virus (Salt shBDNF, n = 8)

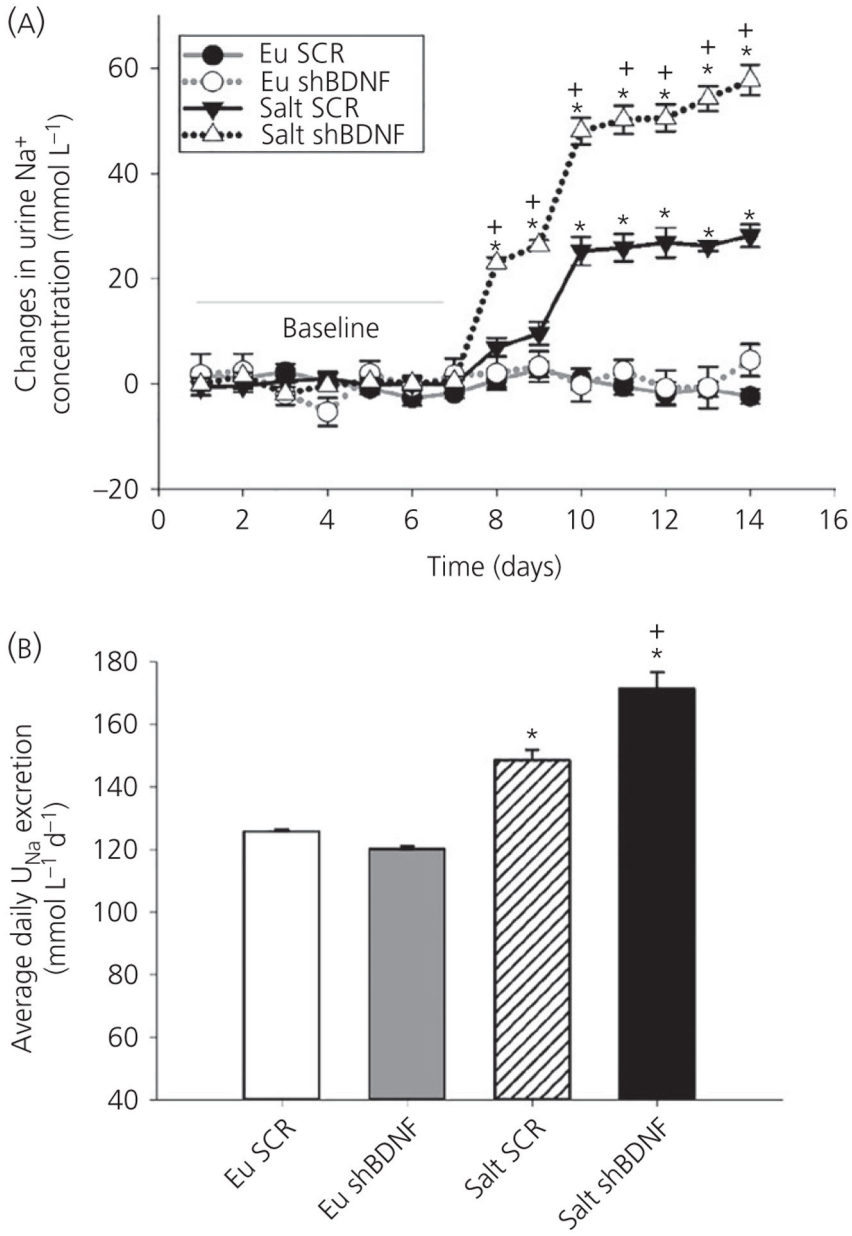

FIGURE 5.

Urine sodium excretion. A, Daily average changes in urine sodium concentration. *$P < 0.05$ vs euhydrated groups (Eu) groups and baseline.$^{+}P < 0.05$ vs Salt scrambled (SCR) B, Average urine sodium excretion during 7 days of salt treatment. Data are the mean ± SEM. *$P < 0.05$ vs Eu groups.$^{+}P < 0.05$ vs Salt SCR. Groups: euhydrated rats injected with SCR virus (Eu SCR, n = 8); euhydrated rats injected with shBDNF virus (Eu shBDNF, n = 8); salt loaded rats injected with SCR virus (Salt SCR, n = 8) and salt loaded rats injected with shBDNF virus (Salt shBDNF, n = 8)

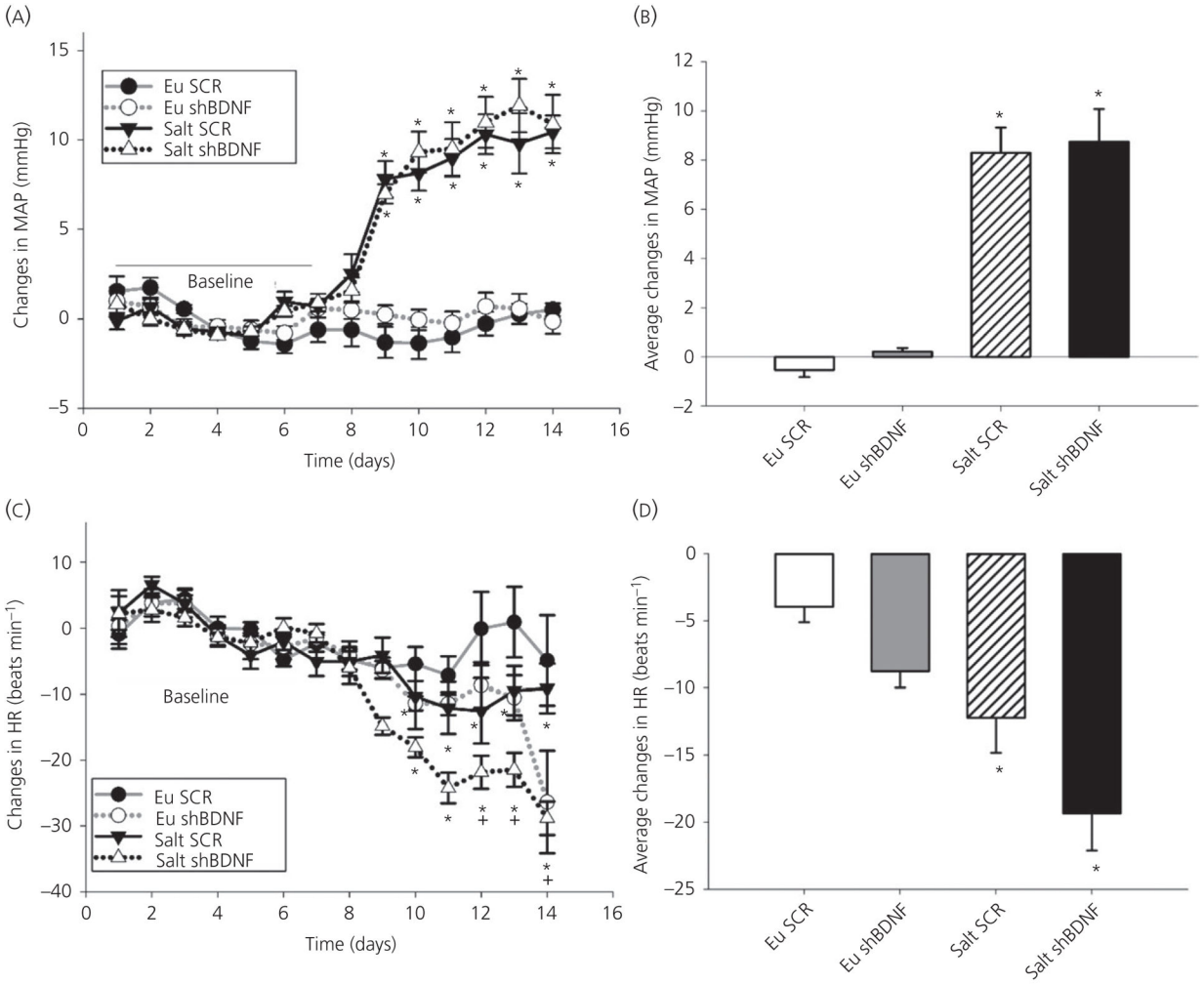

FIGURE 6.

Effect of salt loading and brain-derived neurotrophic factor (BDNF) knockdown in the supraoptic nucleus (SON). A, Daily average changes in mean arterial pressure (MAP). *$P <$ 0.05 vs baseline and euhydrated (Eu) groups. B, Average changes in MAP. *$P < 0.05$ vs Eu groups. C, Daily average changes in heart rate (HR). *$P < 0.05$ vs baseline.$^{+}P < 0.05$ vs Eu scrambled (SCR). D, Average changes in HR. Data are the mean ± SEM. *$P < 0.05$ vs Eu groups. Groups: euhydrated rats injected with scrambled (SCR) virus (Eu SCR, n = 9); euhydrated rats injected with shBDNF virus (Eu shBDNF, n = 9); salt loaded rats injected with SCR virus (Salt SCR, n = 9) and salt loaded rats injected with shBDNF virus (Salt shBDNF, n = 9)

TABLE 1

Primer sequences for quantitative reverse transcriptase-polymerase chain reaction

Gene	Primer sequences
BDNF forward	5’-ATGACCATCCTTTTCCTTACTATGGT-3’
BDNF reverse	5’-TCTTCCCCTTTTAATGGTCAGTGTAC-3’
hnAVP forward	5’-GCCCTCACCTCTGCCTGCTA-3’
hnAVP reverse	5’-CCTGAACGGACCACAGTGGT-3’
S18 forward	5’-CAGAAGGACGTGAAGGATGG-3’
S18 reverse	5’-CAGTGGTCTTGGTGTGCTGA-3’

BDNF, brain-derived neurotrophic factor.

TABLE 2

Plasma osmolality, haematocrit and arginine vasopressin (AVP) concentration in euhydrated rats injected with the control vector (Eu scrambled [SCR]), euhydrated rats injected with shRNA against brain-derived neurotrophic factor (BDNF) (Eu shBDNF), salt loaded rats injected with control vector (Salt SCR) and salt loaded rats injected with shRNA against BDNF (Salt shBDNF) groups

	Eu SCR	**EushBDNF**	**Salt SCR**	**Salt shBDNF**
Osmolality (mOsm kg^{-1})	301.3 ± 1.45 (14)	299.8 ± 1.05 (13)	313.3 ± 1.75 (13)*	305.1 ±0.68 (11)**
Haematocrit *(%)*	42.6 ± 0.53 (14)	41.8 ± 0.64 (13)	47.8 ± 0.74 (13)*	44.4 ± 0.60 (11)**
Plasma AVP (pg ml^{-1})	15.7 ±4.01 (6)	9.3 ± 0.81 (6)	59.9 ± 8.37 (5)*	16.2 ±1.30 (5)**

Values are the mean ± SEM; n, number of rats in each group (in parenthesis).

* $P < 0.05$ vs Control groups.

** $P < 0.05$ vs Salt SCR.

TABLE 3

Absolute mean arterial pressure (MAP) and heart rate in euhydrated rats injected with the control vector (Eu scrambled [SCR]), euhydrated rats injected with shRNA against brain-derived neurotrophic factor (BDNF) (Eu shBDNF), salt loaded rats injected with control vector (Salt SCR), and salt loaded rats injected with shRNA against BDNF (Salt shBDNF) groups

Absolute values	Eu SCR	EushBDNF	Salt SCR	Salt shBDNF
MAP(mmHg)				
Baseline	107.7 ± 0.49 (9)	106.7 ± 0.28 (9)	105.1 ± 0.30 (9)	104.1 ± 0.28 (9)
Treatment	107.2 ± 0.28 (9)	106.9 ± 0.15 (9)	113.5 ± 1.03 (9) *	112.8 ± 1.33 (9) *
Heart rate (beats min^{-1})				
Baseline	387.6 ± 1.23 (9)	385.4 ± 1.05 (9)	378.7 ± 1.86 (9)	379.0 ± 0.73 (9)
Treatment	383.7 ±1.17 (9)	374.1 ± 2.72 (9)	366.5 ± 1.62 (9) **	359.6 ± 2.74 (9) **

Values are the the mean ± SEM; n, number of rats in each group (in parenthesis).

* $P < 0.05$ vs Control groups. No significant difference between Salt SCR and Salt shBDNF groups.

** $P < 0.05$ vs Eu SCR.